Local-Field Effects in the Optical Spectrum of Silicon*

Steven G. Louie,† James R. Chelikowsky, and Marvin L. Cohen
Department of Physics, University of California, Berkeley, California 94720,
and Inorganic Materials Research Division, Lawrence Berkeley Laboratory, Berkeley, California 94720
(Received 13 November 1974)

We have calculated the dielectric response matrix $\epsilon_{\vec{G},\vec{G}'}(\vec{q}=0,\omega)$ for silicon and have obtained the macroscopic frequency-dependent dielectric function. Contrary to recent calculations, local-field corrections do not shift the prominent peak positions of the imaginary part of the dielectric function; further the calculated dielectric function is improved as compared with experiments at higher energies. In particular, agreement with measured energy-loss spectra is significantly better when local-field effects are included.

Recently, much effort has been made to understand the role of microscopic electric fields on various physical properties of crystalline solids.[1-13] Two recent Letters[1,2] have been published on local-field corrections to the optical spectrum of diamond; however, the two calculations give quite different results. By inverting the dielectric response matrix, Van Vechten and Martin,[1] using the pseudopotential method, and Hanke and Sham,[2] using a linear combination of atomic orbitals method, have calculated the macroscopic dielectric function for diamond in the random-phase approximation (RPA).[14] Van Vechten and Martin find that local-field effects shift the strength of the imaginary part of the dielectric function, $\epsilon_2(\omega)$, to the energy region just above the main optical peak. This behavior increases the discrepancy between the calculated $\epsilon_2(\omega)$ and experiment. In an attempt to improve agreement with experiment, Van Vechten and Martin included the effects of dynamical correlation in their calculation of $\epsilon_2(\omega)$ via a one-parameter model. Hanke and Sham, on the other hand, find that local-field effects weaken the strength of $\epsilon_2(\omega)$ in the energy region from the main peak (~12 eV) to 20 eV and that the positions of the prominent peaks in $\epsilon_2(\omega)$ are shifted in the opposite direction to that needed to achieve good accord with experiment by approximately 0.5 eV. Hanke and Sham then include exchange effects (beyond the RPA) in their calculation of the macroscopic dielectric function and are able to achieve better agreement with experiment.

To gain some new insights into the effect of local-field corrections to optical spectra of covalent solids, we present here a calculation of the dielectric function of silicon with local-field effects included. Using an extremely accurate band structure from the empirical pseudopotential method, we have calculated the RPA dielectric response matrix, $\epsilon_{\vec{G},\vec{G}'}(\vec{q}=0,\omega)$, for silicon and inverted it to obtain the macroscopic frequency-dependent dielectric function. We find that (1) local-field corrections do not shift the prominent peak positions of $\epsilon_2(\omega)$ and that (2) local-field corrections do improve the calculated dielectric function as compared with experiments at energies higher than the main optical peak. In particular, agreement with measured energy-loss spectra is significantly better when local-field effects are included.

Within the linear-response theory, a small perturbing electric field of frequency ω and wave vector $\vec{q}+\vec{G}$ in a crystal will establish responses with frequency ω and wave vectors $\vec{q}+\vec{G}'$, where $\vec{G}$ and $\vec{G}'$ are reciprocal-lattice vectors. The microscopic fields of wave vectors $\vec{q}+\vec{G}'$ are generated from the applied perturbing field through umklapp processes. In the case of cubic crystals, the dielectric responses of the solid for longitudinal fields may be described by a matrix in $\vec{G}$ and $\vec{G}'$,[14]

$$\sum_{\vec{G}'}\epsilon_{\vec{G},\vec{G}'}(\vec{q},\omega)E(\vec{q}+\vec{G}',\omega)=E_{\mathrm{pert}}(\vec{q}+\vec{G},\omega), \quad (1)$$

where E is the total field in the crystal and E_{pert} is the applied perturbing field. Microscopic-field effects (or local-field effects) are traditionally ignored by assuming the off-diagonal elements of the dielectric response matrix to be zero. However the off-diagonal elements can be important when considering local-field corrections to optical spectra,[1-3] plasmon dispersion in metals,[4,5] valence-electron density,[6] and lattice dynamics[7-11] in semiconductors and insulators.

In analyzing the optical spectrum, the incident light of frequency ω may be viewed as a perturbing field of vanishingly small wave vector. The macroscopic dielectric function is given by[14]

$$\epsilon(\omega)=\lim_{\vec{q}\to 0}\frac{1}{[\epsilon^{-1}(\vec{q},\omega)]_{\vec{0},\vec{0}}}, \quad (2)$$

where ϵ^{-1} is the inverse of the matrix $\epsilon_{\vec{G},\vec{G}'}$. Adler and Wiser[14] have derived, within the RPA, the following expression for the dielectric response matrix[15]:

$$\epsilon_{\vec{G},\vec{G}'}(\vec{q},\omega)=\delta_{\vec{G},\vec{G}'}-\frac{4\pi e^2}{\Omega|\vec{q}+\vec{G}||\vec{q}+\vec{G}'|}\sum_{\vec{k}nn'}\frac{f_0[E_{n'}(\vec{k}+\vec{q})]-f_0[E_n(\vec{k})]}{E_{n'}(\vec{k}+\vec{q})-E_n(\vec{k})+\hbar\omega+i\hbar\alpha}\langle\vec{k}+\vec{q},n'|\exp[i(\vec{q}+\vec{G})\cdot\vec{r}]|\vec{k},n\rangle$$
$$\times\langle\vec{k},n|\exp[-i(\vec{q}+\vec{G}')\cdot\vec{r}]|\vec{k}+\vec{q},n'\rangle, \quad (3)$$

where Ω is the crystal volume, f_0 is the Fermi-Dirac distribution function, and $|\vec{k},n\rangle$ and $E_n(\vec{k})$ are eigenstates and eigenvalues of the unperturbed Hamiltonian. $\epsilon_{\vec{0},\vec{0}}(\vec{q},\omega)$ is just the usual Cohen-Ehrenreich dielectric function (no local-field effects).[16]

To evaluate the required matrix elements and eigenvalues in Eq. (3), we have calculated a band structure for silicon by using the empirical pseudopotential method.[17] The resulting band structure[18] is in excellent agreement with the optical gaps and photoemission experiments. Each $\epsilon_{G,G'}(\vec{q}=0,\omega)$ was evaluated in energy intervals of 0.125 eV up to 100 eV. The summation over wave vector was performed by evaluating the wave functions and eigenvalues on a grid of 308 $\vec{k}$ points in the irreducible zone. The matrix size of the dielectric response matrix involved in the inversion for Eq. (2) was chosen to be 59×59, containing $\vec{G}$ vectors through the set (222). Symmetry can be invoked to reduce the number of $\epsilon_{\vec{G},\vec{G}'}$ elements which need be calculated to 72. Convergence of the macroscopic dielectric function was confirmed by inversion of $\epsilon_{\vec{G},\vec{G}'}$ including sets of $\vec{G}$ vectors through (111), (200), (220), (311), and (222), respectively.

In order to establish the accuracy of the calculated $\epsilon_{\vec{G},\vec{G}'}$, we have tested our results by using the sum rules as derived by Johnson,[19]

$$\int_0^\infty\omega\,\mathrm{Im}\epsilon_{\vec{G},\vec{G}'}(\vec{q},\omega)\,d\omega=\tfrac{1}{2}\pi\omega_p^2[\rho(\vec{G}-\vec{G}')/\rho(\vec{0})]\hat{e}(\vec{q}+\vec{G})\cdot\hat{e}(\vec{q}+\vec{G}'), \quad (4)$$

where $\omega_p^2=4\pi ne^2/m$ is the plasma frequency, $\rho(\vec{G})$ are the Fourier transforms of the valence-electron density, and $\hat{e}(\vec{q}+\vec{G})$ is a unit vector in the $\vec{q}+\vec{G}$ direction. In Table I we list our calculated results for the specific cases $\vec{G}=\vec{G}'$ and $\vec{G}=0$, $\vec{G}'\neq0$. The integral appearing in Eq. (4) was evaluated over a 100-eV range in intervals of 0.125 eV. Our results demonstrate good internal consistency except for the diagonal elements for the higher $\vec{G}$ vectors. This arises from the facts that $\mathrm{Im}\epsilon_{\vec{G},\vec{G}}(q=0,\omega)$ becomes more extended in frequency as $|\vec{G}|$ increases and that the integrand in Eq. (4) is linearly weighted with frequency. Better results can be obtained if we extend our integrations beyond the 100-eV range. As far as the optical properties are concerned, this high-energy behavior is unimportant, and our values for $\epsilon_{\vec{G},\vec{G}'}$ in the region considered should be very accurate.

TABLE I. Sum rules from Eq. (4) for $\epsilon_{\vec{0},\vec{G}}$ and $\epsilon_{\vec{G},\vec{G}'}$ in units of eV^2 in the limit $\vec{q}\to0$ along the $\hat{x}$ direction.

$\frac{a}{2\pi}\vec{G}$	$\frac{a}{2\pi}\vec{G}'$	$\int\omega\,\mathrm{Im}\epsilon_{\vec{G},\vec{G}'}\,d\omega$	$\frac{\pi}{2}\omega_p^2\frac{\rho(\vec{G}-\vec{G}')}{\rho(0)}\times\hat{e}(\vec{q}+\vec{G})\cdot\hat{e}(\vec{q}+\vec{G}')$
(0,0,0)	(0,0,0)	415.6	433.5
(1,1,1)	(1,1,1)	431.6	433.5
(2,0,0)	(2,0,0)	430.1	433.5
(2,2,0)	(2,2,0)	403.2	433.5
(3,1,1)	(3,1,1)	311.8	433.5
(2,2,2)	(2,2,2)	278.4	433.5
(0,0,0)	(1,1,1)	− 50.9	− 54.7
(0,0,0)	(2,0,0)	0.0	0.0
(0,0,0)	(2,2,0)	11.1	10.3
(0,0,0)	(3,1,1)	21.6	20.2
(0,0,0)	(1,3,1)	7.2	6.7
(0,0,0)	(2,2,2)	15.5	15.0

The calculated imaginary parts of the macroscopic dielectric function with (Adler-Wiser) and without (Cohen-Ehrenreich) local-field corrections, $\epsilon_2(\omega)$ and $\mathrm{Im}\epsilon_{\vec{0},\vec{0}}(\omega)$, respectively, are given in Fig. 1 together with the experimental measurement of Philipp and Ehrenreich.[20] The value for our calculated static dielectric constant without local-field effects is 10.1; with local-field effects it decreases to 9.0. From Fig. 1 we see that local-field corrections do not alter the prominent peak positions, although they do alter the strength of the dielectric function. Compared with the usual $\mathrm{Im}\epsilon_{\vec{0},\vec{0}}(\omega)$, $\epsilon_2(\omega)$ has less strength at energies below the main optical peak, thus increasing the discrepancy with experiment. At energies higher than the main optical peak, the strength of $\epsilon_2(\omega)$ is reduced from that of $\mathrm{Im}\epsilon_{\vec{0},\vec{0}}(\omega)$ until approximately 7 eV. Beyond this point $\epsilon_2(\omega)$ is larger than $\mathrm{Im}\epsilon_{\vec{0},\vec{0}}(\omega)$, an event which must transpire if the well-known sum rules[14] are to be

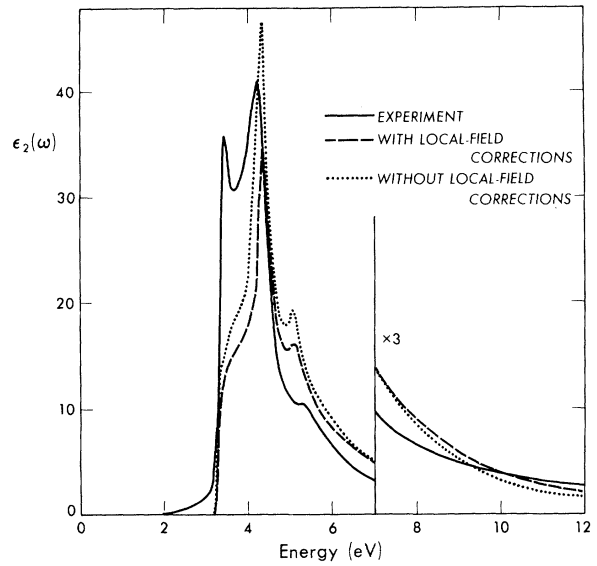

FIG. 1. Calculated $\epsilon_2(\omega)$ for Si, with (dashed curve) and without (dotted curve) local-field effects, compared with experiment (solid curve) from Ref. 20.

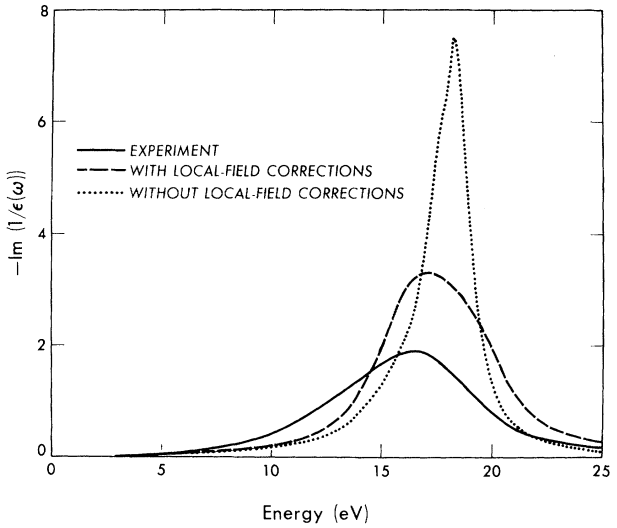

FIG. 2. Calculated energy-loss spectra for Si, with (dashed curve) and without (dotted curve) local-field effects, compared with experiment (solid curve) from Ref. 20.

satisfied. This behavior results in an overall improvement in $\epsilon_2(\omega)$ at higher energies as compared with experiment. Excitonic effects, particularly on the lower-energy side of the main optical peak, which are not included in our calculation, should further improve the agreement between our $\epsilon_2(\omega)$ result and experiment in the low-energy region. The effect of these electron-hole interactions tends to increase the oscillator strength, hence the strength of $\epsilon_2(\omega)$, at the lower energies.[2,21]

Another improvement of $\epsilon(\omega)$ arising from local-field effects at higher energies is reflected in the calculated energy-loss spectrum of silicon as indicated in Fig. 2. We note a drastic decrease in the magnitude of the peak of $\mathrm{Im}[1/\epsilon(\omega)]$ through the inclusion of local-field effects, and a shifting of the peak by approximately 1.2 eV to lower energies.[22] Both these effects result in significantly better agreement with experiments.[20,23] However, effects other than local-field corrections[24] might also be responsible for at least some of the discrepancy between experiment and the calculated $\mathrm{Im}[1/\epsilon^{-1}_{0,0}(\omega)]$.

In conclusion we remark that there are now three calculations on the effect of local-field corrections to the optical spectra of covalent solids using the RPA formalism. All three calculations give different results, indicating that work remains to be done to establish firmly the influences of local-field effects.

We would like to thank Stanley J. Sramek and J. P. Walter for helpful discussions in the early stages of this work. Part of this work was done under the auspices of the U.S. Atomic Energy Commission.

*Work supported in part by the National Science Foundation, Grant No. DMR72-03206-A02.

†National Science Foundation Graduate Fellow.

[1]J. A. Van Vechten and R. M. Martin, Phys. Rev. Lett. 28, 446, 646(E) (1972).

[2]W. R. Hanke and L. J. Sham, Phys. Rev. Lett. 33, 582 (1974).

[3]T. K. Bergstresser and G. W. Rubloff, Phys. Rev. Lett. 30, 794 (1973).

[4]N. H. March and M. P. Tosi, Proc. Roy. Soc., Ser. A 330, 373 (1972).

[5]K. C. Pandey, P. M. Platzman, P. Eisenberger, and E. N. Foo, Phys. Rev. B 9, 5046 (1974).

[6]E. Tosatti, C. Calandra, V. Bortolani, and C. M. Bertoni, J. Phys. C: Proc. Phys. Soc., London 5, L299 (1972).

[7]L. J. Sham, Phys. Rev. 188, 1431 (1969).

[8]R. M. Pick, M. H. Cohen, and R. M. Martin, Phys. Rev. B 1, 910 (1970).

[9]R. M. Martin, Phys. Rev. 186, 871 (1969).

[10]W. R. Hanke, Phys. Rev. B 8, 4585, 4591 (1973).

[11]C. M. Bertoni, V. Bortolani, C. Calandra, and E. Tosatti, Phys. Rev. Lett. 28, 1578 (1972), and Phys. Rev. B 9, 1710 (1974).

[12]D. L. Johnson, Phys. Rev. B 9, 4475 (1974).

[13]J. C. Inkson, J. Phys. C: Proc. Phys. Soc., London

7, 1571 (1974).
[14]S. L. Adler, Phys. Rev. 126, 413 (1962); N. Wiser, Phys. Rev. 129, 62 (1963).
[15]Equation (3) differs from the definition of $\epsilon_{\vec{G},\vec{G}'}$ in Refs. 13 and 14 by a factor $|\vec{q}+\vec{G}|/|\vec{q}+\vec{G}'|$. This definition arises if electric fields are used in Eq. (1) instead of potentials. Both approaches lead to the same macroscopic dielectric function.
[16]H. Ehrenreich and M. H. Cohen, Phys. Rev. 115, 786 (1959).
[17]M. L. Cohen and V. Heine, Solid State Phys. 24, 37 (1970).
[18]J. R. Chelikowsky and M. L. Cohen, Phys. Rev. B. 10, 5095 (1974).
[19]D. L. Johnson, Phys. Rev. B 9, 4475 (1974).
[20]H. R. Philipp and H. Ehrenreich, Phys. Rev. 129, 1550 (1963).
[21]J. C. Phillips, Solid State Phys. 18, 55 (1966).
[22]Our calculated $\mathrm{Im}[1/\epsilon_{\vec{0},\vec{0}}(\omega)]$ differs from that of J. P. Walter and M. L. Cohen, Phys. Rev. B 5, 3101 (1972). Their result yielded a broader peak with a corresponding reduction in peak height. We feel that our result, which involved the use of a more accurate integration scheme for $\mathrm{Im}\epsilon_{\vec{0},\vec{0}}(\omega)$ and did not involve the use of a tail function in obtaining $\mathrm{Re}\epsilon_{\vec{0},\vec{0}}(\omega)$ from $\mathrm{Im}\epsilon_{\vec{0},\vec{0}}(\omega)$, is superior.
[23]H. Dimigen, Z. Phys. 165, 53 (1961).
[24]For example, it is possible that the use of orthogonal-plane-wave matrix elements could also shift the position of the energy-loss peak (M. Schlüter, private communication). Also see J. P. Van Dyke, Phys. Rev. B 5, 1489 (1972).

Experimental Evidence for a Two-Step Process in the Reaction $^{19}F(^{16}O, ^{15}N)^{20}Ne$

F. Pougheon, G. Rotbard, P. Roussel, and J. Vernotte
Institut de Physique Nucléaire, Université Paris-Sud, 91406 Orsay, France
(Received 11 November 1974)

A strong population of the "j-forbidden" 4^+ level at 4.25 MeV in ^{20}Ne is found in the reaction $^{19}F(^{16}O, ^{15}N)^{20}Ne$ at 46-, 58-, and 68-MeV incident energy. It provides evidence for a two-step process. This result was expected for structural and kinematical reasons.

The existence of multistep processes involving core excitation is well known in transfer reactions induced by light particles.[1] In heavy-ion–induced reactions, such multistep processes were expected to be more important (and possibly overwhelming) because core excitation was believed to occur whenever two complex nuclei were close enough for a transfer reaction to take place. Surprisingly, however, no straightforward case was found. Recently, two experiments[2] have indicated the existence of such processes on the basis of angular distribution data, but the clearest evidence would be provided by the direct observation, in the energy spectrum of the outgoing particle, of a transition forbidden by the selection rules of the one-step process. The reaction $^{40}Ca(^{19}F, ^{20}Ne)^{39}K$ was recently reported to be indicative of such a transition,[3] but the result is ambiguous because of an unresolved allowed transition.

In this Letter, we report what we believe to be the first unequivocal evidence for a multistep process, provided by the observation of the forbidden transition to the 4.25-MeV (4^+) level of ^{20}Ne in the reaction $^{19}F(^{16}O, ^{15}N)^{20}Ne$. This result was expected for structural and kinematical reasons which are also outlined.

Consider the $\frac{1}{2}^+ \rightarrow 4^+$ transition in the reaction $^{19}F(^{16}O, ^{15}N)^{20}Ne$. In order to observe this transition, the selection rules for a single-step transfer would require a g component in the wave function of ^{20}Ne. However, the active orbits for this nucleus are usually restricted to the s-d shell and the amplitude of the g component has been estimated[4] to be only about 1 or 2%. On the other hand, the occurrence of this transition via a multistep process was expected for two reasons: Firstly, the very large deformation of the target nucleus should lead to large core excitation. Secondly, heavy-ion–induced transfer reactions are known to be subject to a strong Q, l, and j dependence[5] resulting from kinematical matching conditions. The same semiclassical analysis[6] which describes these matching conditions for a single-step transfer can be applied to the transfer involved during a multistep process.[7] Transfers to the $d_{5/2}$, $s_{1/2}$, or $d_{3/2}$ orbits can connect, separately or together, the four first members of the ground-state rotational band of ^{19}F to the 4^+ level of ^{20}Ne. It can be shown that several of the transfers with a large spectroscopic factor are also favored by good kinematical matching conditions.

The reaction $^{19}F(^{16}O, ^{15}N)^{20}Ne$ was studied with